

A theoretical study of the luminosity temperature relation for clusters of galaxies

A. Del Popolo¹, N.Hiotelis² & J. Peñarrubia³

ABSTRACT

A luminosity-temperature relation for clusters of galaxies is derived. The two models used, take into account the angular momentum acquisition by the proto-structures during their expansion and collapse. The first one is a modification of the self-similar model (SSM) while the second one is a modification of the Punctuated Equilibria Model (Cavaliere et al. 1999). In both models the mass-temperature relation (M-T) used is based on the calculations of Del Popolo (2002b).

We show that the above models lead, in X-rays, to a luminosity-temperature relation that scales as $L \propto T^5$, at scale of groups, flattening to $L \propto T^3$ for rich clusters and converging to $L \propto T^2$ at higher temperatures. However a fundamental result of our paper is that the non-similarity in the L-T relation, can be explained by a simple model that takes into account the amount of the angular momentum of a proto-structure. This result is in disagreement with the widely accepted idea that the above non-similarity is due to non-gravitating processes as those of heating/cooling.

Subject headings: cosmology: theory - large scale structure of universe - galaxies: formation

1. Introduction

Observations of clusters of galaxies (e.g, ROSAT, ASCA), performed in the past decade, have shown the existence of a tight correlation between the total gravitating mass of clusters, M_{tot} , their X-ray luminosity (L_X), and temperature (T_X) of the intra-cluster medium (ICM) (David et al. 1993; Markevitch 1998; Horner, Mushotzky & Sharf 1999 (hereafter

¹Boğaziçi University, Physics Department, 80815 Bebek, Istanbul, Turkey

²First Experimental Lyceum of Athens, Ipitou 15, Plaka 10557, Athens, Greece

³Astronomisches Rechen-Institut, Mñchhofstrasse 12-14, D-69120 Heidelberg, Germany

HMS)). The importance of these relations is due to the fact that cluster masses are difficult to measure directly, and when comparing cluster observations with models of structure formation a surrogate for cluster mass is used. Since M_{tot} compares with the ICM temperature measurements which can be obtained through X-ray spectroscopy, this explains the importance of an M-T relation. On the one hand, the X-ray temperature measures the depth of the potential wells, and the bolometric luminosity, $L \propto n^2 R_X^3 T^{1/2}$, emitted as thermal bremsstrahlung by intra-cluster plasma measures the baryon number density, n within the volume R_X^3 . Till some years ago, the cluster structure was considered to be scale-free, which means that the global properties of clusters, such as halo mass, luminosity-temperature, and X-ray luminosity would scale self-similarly (Kaiser 1986). In particular, the gas temperature would scale with cluster mass as $T \propto M^{2/3}$ and the bolometric X-ray luminosity would scale with temperature as $L \propto T^2$, in the bremsstrahlung-dominated regime above ~ 2 keV. ⁴

Studies following that of Kaiser (1986) showed that the observed luminosity-temperature relation is closer to $L \propto T^3$ (e.g., Edge & Stewart 1991), indicating that non-gravitational processes should influence the density structure of a cluster’s core, where most of the luminosity is generated (Kaiser 1991; Evrard & Henry 1991; Navarro, Frenk & White 1995; Bryan & Norman 1998). One way to obtain a scaling law closer to the observational one is to have non-gravitational energy injected into intra-cluster medium (ICM) before or during cluster formation. This solution, called pre-heating, was originally invoked to solve two related problems: a) to explain (Kaiser 1991; Evrard & Henry 1991) ⁵ the apparent negative evolution of the X-ray cluster luminosity function (Gioia et al. 1990; Henry et al. 1992) from the Einstein Medium Sensitivity Survey in a $\Omega_m = 1$ Universe ; b) to explain (White 1991) ⁶ why groups and low-mass clusters seem to have higher X-ray temperatures than expected based on member velocity dispersions.

The mechanisms proposed to explain the slope change of the L-T relation can be divided into three main categories:

(i) models that include a pre-heating of the gas within a cluster. Ponman et al. (1999) showed that the entropy of the ICM in the centre of low-temperature clusters is greater than the value expected from gravitational collapse. It has been shown that models that include an additional gas entropy can successfully reproduce many observational properties

⁴Indeed, numerical simulations that include gas dynamics but exclude non-gravitational processes such as radiative cooling and supernova heating produce clusters that obey these scaling laws (e.g., Evrard, Metzler, & Navarro 1996; Bryan & Norman 1998; Thomas et. al 2001b).

⁵Kaiser’s self similar model predicts $L \propto T^{3.5}$. Evrard & Henry (1991) obtained the relation $L \propto T^{11/4}$

⁶In this case pre-heating was in form of supernovae-driven galactic winds

(Bower et al. 1997; Cavaliere et al. 1997, 1999; Tozzi & Norman 2001; Borgani et al. 2001; Voit & Bryan 2001).

(ii) models that implement feed-back processes that alter the gas characteristics during the evolution of the cluster. In principle, there are many different physical processes that could break the self-similar scaling, including heating from SN or from AGN, or the removal of low-entropy gas via radiative cooling with subsequent supernova heating (Voit & Bryan 2001). Another example is that of Muanwong et al. (2001), who simulated galaxy cluster formation including radiative cooling with cool gas dropout and was able to reproduce the $L \propto T^3$ dependence, without adding any entropy to the gas. Moreover other possibilities, such as magnetic pressure or cosmic-ray pressure have not been ruled out. Allen & Fabian (1998) have examined the effects of cooling flows for a sample of the most X-ray luminous ($L_{\text{Bol}} > 10^{45}$ erg/s) finding a flattening from $L \propto T^3$ to $L \propto T^2$ in agreement with models that include the effects of shocks and pre-heating on the X-ray gas (Cavaliere et al. 1997, 1999). Cavaliere et al. (1997, 1998), have constructed a model in which the observed L-M relation on both cluster and group scales can be reproduced by varying the gas density at the virial radius, according to the accretion-shock strength, as determined by the temperature difference between the infalling and virialised gases. Another possibility to explain the L-T relation are systematic variations in the baryonic fraction with cluster mass (David et al. 1993). To distinguish among these processes, **observations of high-redshift groups and clusters will be crucial to measure the evolution of the observed scaling relations as function of redshift**.

(iii) hydro-dynamical models that do not include gas pre-heating, nor feed-back processes, which also reproduce the available observational data (e.g., Bryan & Norman 1998). Throughout this paper, we will analyse this last scenario.

On the other hand, the mass-temperature relation, seemed like it ought to be more fundamental and less sensitive to non-gravitational effects. Yet, observations collected over the last few years indicate that this relation also disagrees with both the scale-free predictions and simulations that exclude non-gravitational processes (Horner, Mushotzky, & Scharf 1999; Nevalainen, Markevitch, & Forman 2000 (hereafter NMF); Finoguenov, Reiprich, & Böhringer 2001 (hereafter FRB); Xu, Jin, & Wu 2001). These results derive mostly from resolved X-ray and temperature profiles coupled with the assumption of hydrostatic equilibrium, **and** they do seem consistent with gravitational lensing measurements (Allen, Schmidt, & Fabian 2001). Understanding the scaling properties of clusters is of broad importance because these scaling laws are integral to determination of cosmological parameters. Thus, any inaccuracies in the mass-temperature relation propagate into uncertainties in cosmological parameters derived from clusters (**e.g., Voit 2000, hereafter V2000**).

In Del Popolo (2002b), we derived the mass-temperature relation and its time evolution

for clusters of galaxies in different cosmologies. **We use** two different models: the first one is a modification and improvement of a model by Del Popolo & Gambera (1999), based upon a modification of the top-hat model in order to account **for** angular momentum acquisition by proto-structures and for an external pressure term in the virial theorem. The second one is an improvement of a model proposed by V2000, **again to account for the angular momentum acquired by proto-structures during their formation.** Both models showed that the M-T relation is not self-similar. A break is present in the quoted relation at $T \sim 3\text{keV}$ and, at the lower mass end, the power law index of the M-T relation is larger than $\alpha = 3/2$ even in flat universes. The slope of the power-law index depends on the considered cosmology. The two models also agree in predicting a more modest time evolution of the quoted relation in comparison with the results of previous models, **which also depends on the cosmology.**

This is in agreement with studies showing that the self-similarity in the M-T relation seems to break at some keV (NMF; Xu, Jin & Wu 2001). By means of ASCA data, using a small sample of 9 clusters (6 at 4 keV and 3 at ~ 1 keV), NMF has shown that $M_{\text{tot}} \propto T_X^{1.79 \pm 0.14}$ for the whole sample, and $M_{\text{tot}} \propto T_X^{3/2}$ excluding the low-temperature clusters. Xu, Jin & Wu (2001) has found $M_{\text{tot}} \propto T_X^{1.60 \pm 0.04}$ (using the β model), and $M_{\text{tot}} \propto T_X^{1.81 \pm 0.14}$ by means of the Navarro, Frenk & White (1995) profile. FRB have investigated the T-M relation in the low-mass end finding that $M \propto T^{\sim 2}$, and $M \propto T^{\sim 3/2}$ at the high mass end. This behaviour has been attributed to the effect of the formation redshift (FRB) (but see Mathiesen 2001 for a different point of view), or to cooling processes (Muanwong et al. 2001) and heating (Bialek, Evrard & Mohr 2000). Afshordi & Cen (2001) (hereafter AC) have shown that non-sphericity introduces an asymmetric, mass dependent, scatter for the M-T relation altering its slope at the low mass end ($T \sim 3$ keV).

The L-T and M-T relations are somehow related: as shown by Shimizu et al. (2003), it is possible to make a reliable prediction for the L - T relation once the M - T relation is specified. In turn, one can obtain the M - T relation that reproduces the observed L - T relation without assuming an ad hoc model for the thermal evolution of intra-cluster gas. The two relations (M-T and L-T) are strictly connected, as shown by Shimizu et. al (2003).

This conclusion in turn indicates that the L - T relation provides a good diagnosis of the underlying M - T relation, which is as yet poorly determined observationally.

Apart from the physical mechanism of the additional thermal processes, there are three **effects** that might modify the mass dependence of X-ray luminosity and steepen the resulting L - T relation. First, the gas density profile might be significantly flatter for less massive systems. Second, the mass dependence of the hot gas mass fraction is strong as $f_{\text{gas}} \propto M_{\text{vir}}^{1/3}$. Finally, the mass-temperature relation is $T_{\text{gas}} \propto M_{\text{vir}}^{2/5}$. In practice, a realistic model should be a combination of those three effects to some extent.

In this paper we derive a luminosity-temperature relation for clusters of galaxies that takes into account the amount of the angular momentum of proto-structures. We use two different models: the first (that we call MSSM) is a modification of the self-similar model (SSM) while the second one is a modification of the Punctuated Equilibria Model (hereafter MPPEM) (Cavaliere et al. 1999). We show that the presence of the angular momentum during the gravitational collapse leads to non-self similar L-T relation. The two models used are described in Sect. 2. The results are presented and discussed in Sect. 3 and the conclusions are summarised in Sect.4.

2. Model

2.1. Modified Self-Similar model for the L-T relation

The L-T relation constitutes a fundamental link between the physics of the baryon component and the dynamical properties of the Dark Matter condensations. The simplest model describing **that** relation is the SSM model (Kaiser 1986), obtained assuming that the gas density or the baryon number density, n , is proportional to the average Dark Matter density, ρ , and that the virial radius, R_{vir} is proportional to R_X (see introduction for a definition). In this way, one obtains, according to this last, $L \propto M_{\text{vir}} \rho T^{1/2}$. In fact, $T \propto M_{\text{vir}}/R_{\text{vir}}$, $n \propto \rho \propto M_{\text{vir}}/R_{\text{vir}}^3$, $R_{\text{vir}} \propto R_X$ and $L \propto \int_0^{R_{\text{vir}}} \rho^2 T^{1/2} r^2 dr \propto \rho^2 T^{1/2} R_{\text{vir}}^3$, and recalling that $R_{\text{vir}} \propto (M_{\text{vir}}/\rho)^{1/3}$, leads to $L \propto \rho M_{\text{vir}} T^{1/2}$ or recalling that $R_{\text{vir}} \propto (T/\rho)^{1/3}$, we get $L \propto \rho^{1/2} T^2$. This last result is inconsistent with observed correlation close to $L \propto T^3$ (Edge & Stewart 1991; Mushotzky 1994). Additionally, a further steepening at the temperature of galaxy groups is indicated for thermal emission not associated with single galaxies (Ponman et al. 1996).

In the following, we derive a modified SSM, showing that slope of the L-T relation changes at different scales.

Using Balogh et al (1999) notation, let us begin with a cluster with gas temperature $T(r)$, density profile $\rho(r)_g$, for which the bolometric X-ray luminosity from Bremsstrahlung scales as:

$$L = \frac{6\pi k}{C_1(\mu m_p)^2} \int_0^{R_{\text{vir}}} r^2 \rho_g(r)^2 T_g(r)^{1/2} dr \quad (1)$$

(see Balogh et al. 1999), where $C_1 = 3.88 \times 10^{11} \text{ s K}^{-1/2} \text{ cm}^{-3}$, $\mu = 0.59$, $R_{\text{vir}} \propto (M_{\text{vir}}/\rho)^{1/3}$ is the virial radius where $\rho(z) \propto (1+z)^3$ is the Dark Matter (DM) density in the cluster, proportional to the average cosmic DM density ρ_u at formation. The simplest model describing the L-T relation, that can be calculated by Eq. (1), is the SSM (Kaiser 1986), assuming that

the $\rho_g \propto \rho$.

We only consider haloes in which not all of the gas within R_{vir} has had time to cool since the halo formed.

We assume a singular, truncated isothermal sphere for the dark matter potential, $\rho(r) = \rho_R(r/R_{\text{vir}})^{-2}$, where ρ_R is the density at the virial radius, R_{vir} , and is equal to a third of the mean density *within* R_{vir} , $\bar{\rho}(R_{\text{vir}})$. This latter quantity is related to the critical density at redshift z by $\bar{\rho}(R_{\text{vir}}) = \Delta_c(z)\rho_c(z)$, and $\Delta_c = 78\Omega(z) + 80 + 300\Omega(z)/(1 + 15\Omega(z))$ is a fit, accurate to better than 2 per cent, to the results of the spherical collapse model as presented in Eke et al. (1996). It will be convenient to define a redshift evolution term, $F_1(z)^2 = (1+z)^2(1+\Omega_o z)\Delta_c(z)/\Delta_c(0)$, so that

$$\rho_R = \frac{1}{3}\Delta_c(0)\rho_c(0)F_1(z)^2. \quad (2)$$

For $\Omega_o = 1$, $F_1(z)^2 = (1+z)^3$ and $\Delta_c = 178$. In this model, we make the common assumption (e.g., Eke et al. 1996) that the gas is distributed isothermally, with a temperature equal to the virial temperature of the halo. If the gas is dissipationless, its density profile will match that of the dark matter, i.e.,

$$\rho_g(r) = \rho_{g,R}(r/R_{\text{vir}})^{-2}, \quad (3)$$

and $\rho_{g,R}/\rho_R = \Omega_b/\Omega_o$. To avoid the singularity at $r = 0$ when integrating over the assumed isothermal profile, an arbitrary core radius of $r_c = f_c R_{\text{vir}}$ is adopted with $f_c = 0.1$, such that $\rho_g(r < r_c) = \rho_g(r_c)$. The integral in Eq. (1) is dominated by the contribution from within a few core radii, and thus the scaling properties of this integral depend weakly on the assumed density profile. Furthermore, departures from the standard profile can be accommodated by redefining the core radius of the system.

In order to obtain the luminosity–mass relation, we evaluate Eq. (1) and use the M-T relation, which takes into account the angular momentum of the proto-structure, obtained in Appendix A:

$$kT \simeq 8keV \left(\frac{M^{\frac{2}{3}}}{10^{15}h^{-1}M_{\odot}} \right) \frac{\left[\frac{1}{m_1} + \left(\frac{t_{\Omega}}{t} \right)^{\frac{2}{3}} + \frac{K_1(m_1, x)}{M^{8/3}} \right]}{\left[\frac{1}{m_1} + \left(\frac{t_{\Omega}}{t_0} \right)^{\frac{2}{3}} + \frac{K_0(m_1, x)}{M_0^{8/3}} \right]} \quad (4)$$

where $K_1(m_1, x)$ ⁷ is given by:

$$K_1(m_1, x) = (m_1 - 1)FxLerchPhi(x, 1, 3m_1/5 + 1) -$$

⁷ $K_0(m_1, x)$ indicates that $K_1(m_1, x)$ must be calculated assuming $t = t_0$

$$(m_1 - 1) F \text{LerchPhi}(x, 1, 3m_1/5) \quad (5)$$

and

$$F = \frac{2^{7/3} \pi^{2/3} \xi \rho_b^{2/3}}{3^{2/3} H^2 \Omega} \int_0^r \frac{\mathcal{L}^2 dr}{r^3} \quad (6)$$

$m_1 = 5/(n + 3)$, $t_\Omega = \frac{\pi \Omega_0}{H_o(1-\Omega_0-\Omega_\Lambda)^{3/2}}$, $x = 1 + (\frac{t_\Omega}{t})^{2/3}$ which is connected to mass by $M = M_0 x^{-3m_1/5}$ (V2000) and $\xi = \frac{r_{ta}}{x_1}$, where r_{ta} is the turn-around radius and x_1 is defined by the relation $M = \frac{4\pi \rho_b x_1^3}{3}$ with ρ_b is the background density. Finally we get:

$$L = 3.31 \times 10^{45} \left(\frac{M}{M_o} \right)^{4/3} \left(\frac{1}{178} \Delta_c \right) F_1^2 \left(\frac{\Omega_b}{\Omega} \right)^2 \sqrt{\frac{\frac{1}{m_1} + \left(\frac{t_\Omega}{t} \right)^{2/3} + \frac{K_1(m_1, x)}{\left(\frac{M}{M_o} \right)^{8/3}}}{\frac{1}{m_1} + \left(\frac{t_\Omega}{t} \right)^{2/3} + \frac{K_0(m_1, x)}{M_o^{8/3}}}} \left(\frac{1 - fc}{fc} \right) \quad (7)$$

which differently from Kaiser's (1986) prediction is not self-similar. It reduces to the self-similar form ($L \propto M^{4/3}$) if angular momentum acquisition is not taken into account, namely if $\mathcal{L} \rightarrow 0$ (or $F \rightarrow 0$).

The previous computation depends on the value of the angular momentum acquired by the DM haloes from tidal torques from surrounding matter. This enters the L-T relation through the quantities F and K_1 (see also Appendix A). In the limit of vanishing angular momentum the L-T and the M-T relations reduce to the well-known self-similar forms. Then, it is important to add a discussion on the magnitude of the angular momentum calculated as in previous papers (e.g., Del Popolo & Gambera 1998; Del Popolo et al. 2001).

The angular momentum is acquired by the cosmological torque acting on the proto-structures due to the tidal field of the environment. The amount of angular momentum as well as its distribution are related to the assumed power spectrum of density perturbations. We have to note here that the problem of the growth of angular momentum of proto-structures from the tidal torques of the surrounding matter has been studied extensively in the literature with both analytical and numerical (N-body) methods (e.g. Efstathiou & Jones 1979; Barnes & Efstathiou 1987; Voglis & Hiotelis 1989; Warren et al. 1992; Eisenstein & Loeb 1995; Kratsov et al. 1998). A main result of the above studies is that the values of the dimensionless spin parameter $\lambda \equiv \mathcal{L}|E|^{1/2}/GM^{5/2}$, (Peebles 1971), follow a log-normal distribution with a small average value 0.05. In the above relation \mathcal{L} is the total angular momentum of the proto-structure, E is its binding energy, M its mass and G the gravitational constant. The above numerical results are confirmed by analytical studies presented by other authors as those of Steinmetz & Bartelmann (1995) and Catelan & Theuns (1996). To be more precise, λ depends on the galactic morphological type, being as high as $\lambda \simeq 0.5$

for spirals and SO galaxies, and $\lambda \simeq 0.05$ for ellipticals, although the dispersion around these values is large (Efstathiou & Jones 1979). In the case of structures of $10^{12} - 10^{13}$ its value is $\simeq 0.1$ and $\simeq 0.01$ for clusters ⁸.

In this paper, we calculated angular momentum as Sect. 3 in Del Popolo et al. (2001), following Eisenstein & Loeb (1995). With the Bardeen et al. (1986) power spectrum smoothed on galactic scale for a $\nu = 2$ peak, the model gives a value of $2.5 \times 10^{74} \text{gcm}^2/\text{s}$, in very good agreement with Catelan & Theuns (1996), in other words the amount of angular momentum used in our calculations is consistent with the values of λ predicted by the tidal fields of the surrounding matter. Although this amount is in general small, our results show that **it** is efficient to lead to a non-similar L-T relation. **The angular momentum of dark matter haloes** has also **other important consequences**. For example small amounts of angular momentum are able to change the density profile of dark matter haloes from the isothermal law $\rho(r) \propto r^{-2}$ to a profile that it flattens significantly inwards, (e.g. Hiotelis 2002).

Moreover, several studies have shown that the influence and the role of shear on structure formation is of fundamental importance. Shear on a density perturbation can be produced by the intrinsic asphericity of the perturbation itself (internal shear) or it can be due to the interaction of the perturbation with the neighbouring ones (external shear). For example, according to the previrialization conjecture (Peebles & Groth 1976, Davis & Peebles 1977, Peebles 1990), initial asphericities and tidal interactions between neighbouring density fluctuations induce significant non-radial motions which oppose the collapse. This means that virialized clumps form later, with respect to the predictions of the linear perturbation theory or the spherical collapse model, and that the initial density contrast, needed to obtain a given final density contrast, must be larger than that for an isolated spherical fluctuation. This kind of conclusion was supported by Barrow & Silk (1981), Szalay & Silk (1983), Villumsen & Davis (1986), Bond & Myers (1993a,b) and Lokas et al. (1996). Arguments based on a numerical least-action method lead Peebles (1990) to the conclusion that irregularities in the mass distribution, together with external tides, induce non-radial motions that slow down the collapse. In a more recent paper, Audit et al. (1997) they conclude that spherical collapse is the fastest. This result is in agreement with Peebles (1990), and more recent papers, namely Del Popolo et al. (2001), Del Popolo (2002a).

⁸The resulting typical circular velocities of structures is $\simeq 150 \text{km/s}$ for galaxies similar to the Milky Way, $\simeq 5 \text{ km/s}$ for clusters and $\simeq 10 \text{ km/s}$ for superclusters (see Catelan & Theuns 1996)

2.2. Improvements to the punctuated equilibria model

In this subsection, we shall extend the punctuated equilibria model (PEM) by Cavaliere, Menci e Tozzi (1997, 1998, 1999) (hereafter CMT97, 98, 99) to take account of angular momentum acquisition from the proto-structure. In their model (CMT98), the cluster evolution is described as a sequence of “punctuated equilibria” (PE), that is to say, a sequence of hierarchical merging episodes of the DM halos, associated in the ICP to shocks of various strengths (depending on the mass ratio of the merging clumps), which provide the boundary conditions for the ICP to readjust to a new hydrostatic equilibrium.

The X-ray bolometric luminosity of a cluster is given by Eq. (1), which in CMT98 notation is:

$$L \propto \int_0^{r_2} n^2(r) T^{1/2}(r) d^3r . \quad (8)$$

Here $T(r)$ is temperature in the plasma and r_2 is the cluster boundary, that we take to be close to the virial radius $R_{\text{vir}} \propto M_{\text{vir}}^{1/3} \rho^{-1/3}$, where $\rho(z) \propto (1+z)^3$ is the DM density in the cluster, proportional to the average cosmic DM density $\rho_u(z)$ at formation.

As shown in Appendix B, the L-T relation can be casted in the form:

$$L \propto \left(\frac{n_2}{n_1}\right)^2 \rho \left[\frac{T_2}{T_v}\right]^{1/2} \frac{1}{[n(r)/n_2]^{2+(\gamma-1)/2} m^{4/3}} \sqrt{\frac{\frac{1}{m_1} + \left(\frac{t_\Omega}{t}\right)^{2/3} + \frac{K_1}{\left(\frac{m}{m_0}\right)^{8/3}}}{\frac{1}{m_1} + \left(\frac{t_\Omega}{t}\right)^{2/3} + \frac{K_0}{m_0^{8/3}}}} \quad (9)$$

See Appendix B for a derivation of Eq. (9) and a definition of the terms involved.

Our final aim is to compute the average value of L and its dispersion, associated with a given cluster mass m .

In order to reach this goal, we must sum over the shocks produced at a time $t' < t$ in all possible progenitors m' (weighting with their number) by the accreted clumps Δm (weighting with their merging rate); finally, we integrate over times t' from an effective lower limit $t - \Delta t$.

The average L is then given by

$$\langle L \rangle = Q \int_{t-\Delta t}^t dt' \int_0^m dm' \int_0^{m-m'} d\Delta m \frac{df}{dm'}(m', t' | m, t) \frac{d^2 p(m' \rightarrow m' + \Delta m)}{d\Delta m dt'} L ; \quad (10)$$

and the variance is given by

$$\langle \Delta L^2 \rangle = Q \int_{t-\Delta t}^t dt' \int_0^m dm' \int_0^{m-m'} d\Delta m \frac{df}{dm'}(m', t' | m, t) \frac{d^2 p(m' \rightarrow m' + \Delta m)}{d\Delta m dt'} \left(L - \langle L \rangle \right)^2 . \quad (11)$$

where Q is the normalisation factor (the compounded probability distribution in Eqs. (10) and (11) has been normalised to 1. The effective lower limit for the integration over masses is set as described in Sect. (2.4) of CMT99.

3. Results

The results of our calculation are plotted in Fig. 1-3.

In Fig. 1, we plot a direct comparison between the SSM, long-dashed line, with the MSSM, short dashed line, with the PEM ⁹, solid line, and finally with the MPEM with a tilted CDM cosmogony. As well known, the SSM predicts that $L \propto T^2$ (Kaiser 1986), while the MSSM predicts non self-similar behaviour of the L-T relation: namely a L-T relation $L \propto T^5$ at scale of groups, $L \propto T^3$ for rich clusters in agreement with observations and the L-T relation saturates toward $L \propto T^2$ for higher temperatures. The plot shows that the MSSM predicts a similar behaviour of the L-T relation to that predicted by the PEM. Differences of maximum 10% are noted for smaller values of the temperature.

It is noticed above, that a self-similar evolution for all clusters, at typical cluster temperatures ($T > 2$ keV), should lead to $L \propto T^2$, since free-free emission dominates the cooling. Instead the observed L-T relation is more steep, $L \propto T^{2.6-2.9}$, meaning that lower temperature clusters and groups of galaxies are far less luminous than expected. Several different models have been proposed in order to explain the quoted behaviour in the L-T relation. The key-point of these models is that the X-ray luminosities of low-temperature clusters are small because their gas is less centrally concentrated than in hotter clusters, an effect that has been attributed to an universal minimum entropy level in intra-cluster gas, resulting from supernova heating (Ponman et al. 1999; Wu et al. 2000; CMT99), from heating by active nuclei (Wu et al. 2000) or from radiative cooling (Wu et al. 2000; Bryan 2001; Pearce et al. 2000). In other terms for some reasons the core gas is less high than that

⁹The PEM is based on hierarchical clustering. Group and cluster formation is envisaged in terms of DM potential wells evolving hierarchically, and engulfing outer baryons by accretion of smooth gas or by merging with other clumps. After a merging episode, the ICP in the wells falls back to a new, approximate hydrostatic equilibrium. This sequence of hydrostatic equilibria of the ICP is physically motivated for all merging events except for those involving comparable clumps (a mass ratio larger than $\sim 1/4$). However these sum up to less than 10% in the number. In the PEM, thermal energy of the infalling gas is initially due to stellar pre-heating (of nuclear origin); then it is increased to the virial value (of gravitational origin) when the accreted gas is bound in DM sub-clumps. So the pre-heating sets an effective threshold $kT_1 \sim 0.5$ keV to gas inclusion, which breaks the self-similar correlation $L \propto T^2$ not only in its vicinity but also up to a few keV.

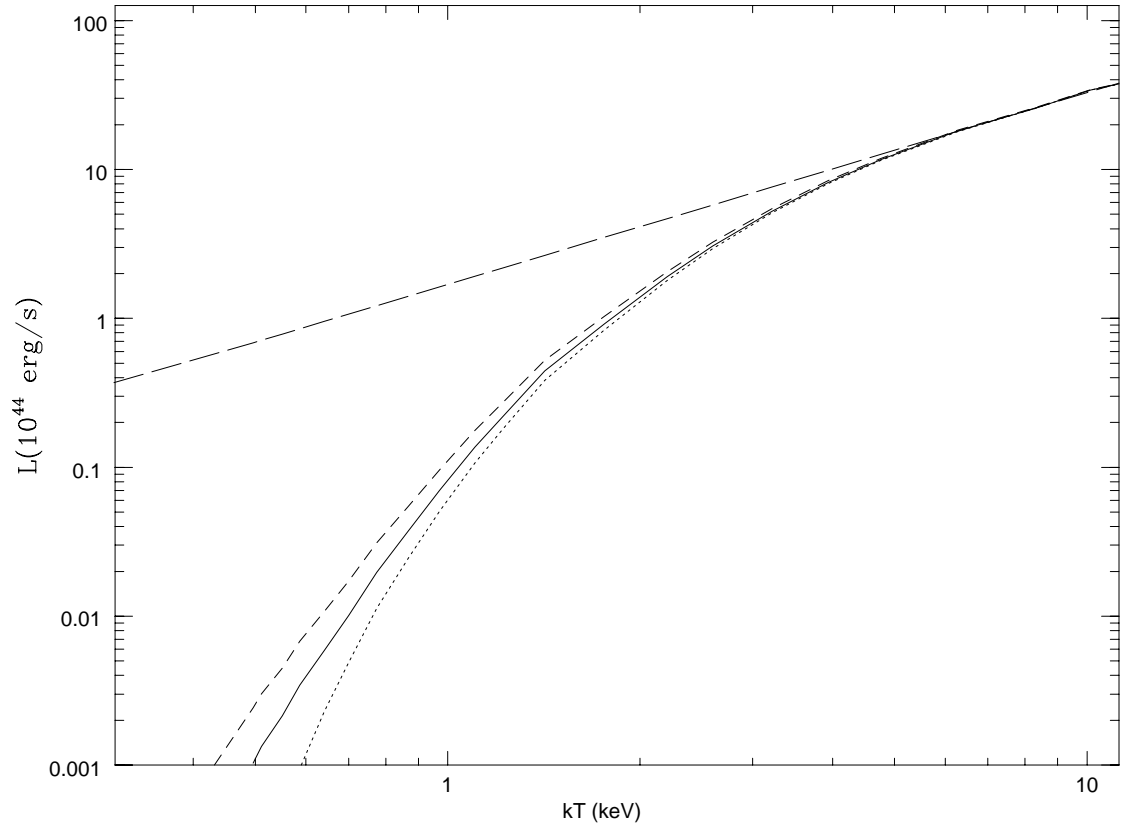


Fig. 1.— Comparison between the SSM, long-dashed line, with the MSSM, short dashed line, the PEM solid line, and MPEM dotted line.

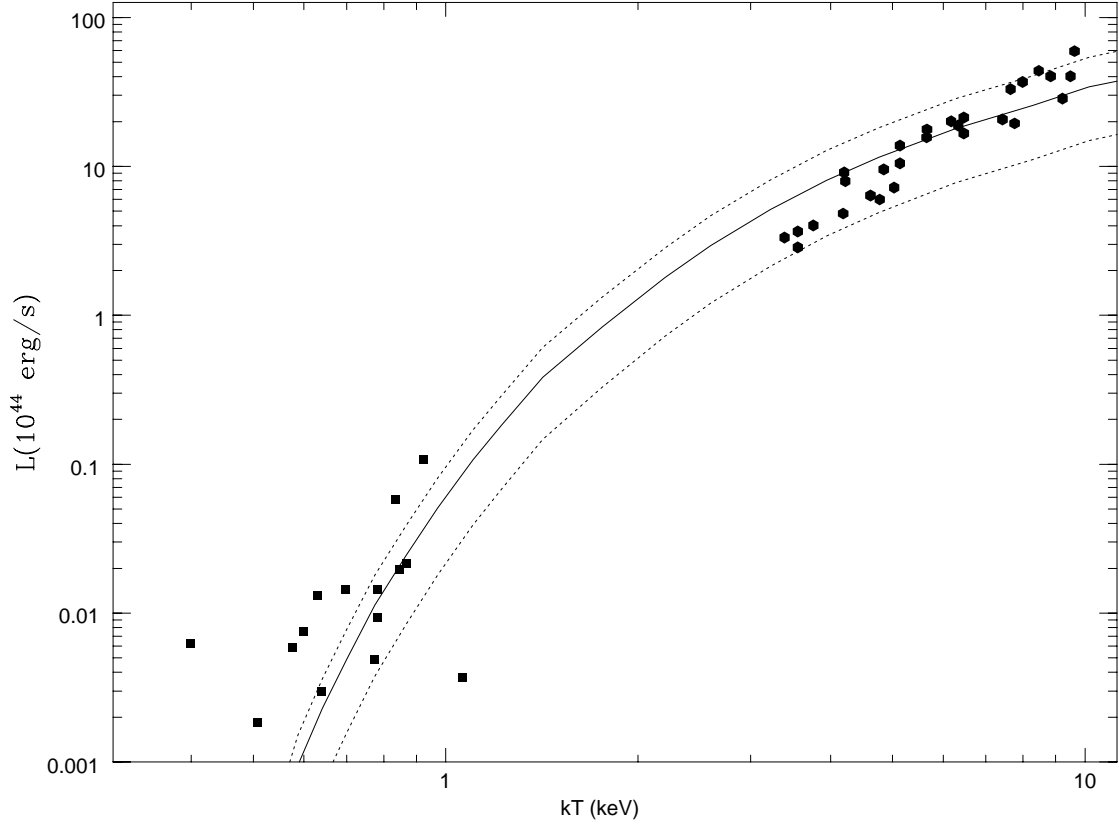


Fig. 2.— MPEM model: the average L-T correlation with the 2σ dispersion (dotted lines), for a tilted cosmogony. Group data from Ponman et al. (1996) are represented by solid squares while cluster data from Markevitch (1998) are represented by solid hexagons.

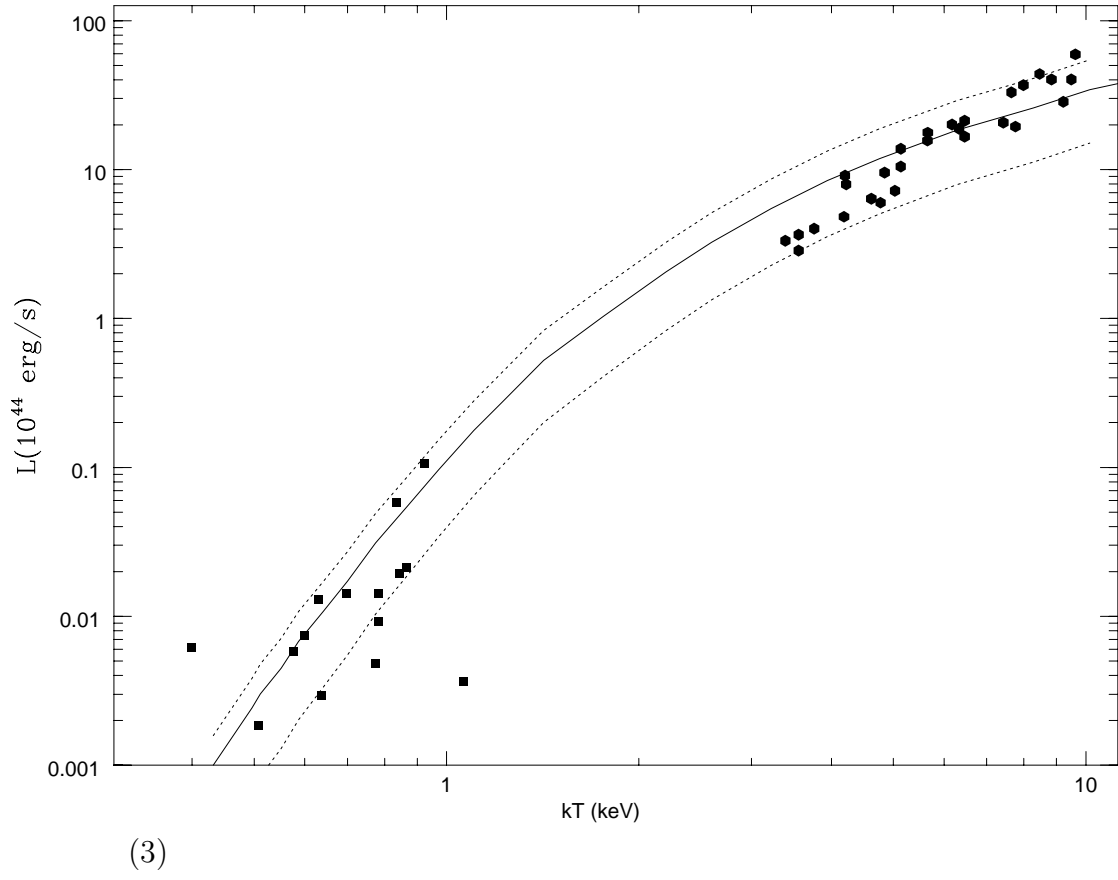


Fig. 3.— Similar to Fig. 2 but for the MSSM model.

expected in the self-similar model. For example, an early episode of uniformly distributed supernova feedback, could rectify the problem by heating the un-condensed gas and therefore making it harder to compress in the core. In other words, the models with pre-heating and similar gives rise to the quoted break because they change the density in the core. During the hierarchical buildup an energy input pre heats the gas before it falls into new groups and clusters, so hindering its flow into the latter. The core density shall decrease and so the luminosity.

A similar mechanism acts in the model of this paper. In fact, as shown in Del Popolo & Gambera (1998), the angular momentum acquired by a shell centred on a peak in the CDM density distribution is anti-correlated with density: high-density peaks acquire less angular momentum than low-density peaks (Hoffman 1986; Ryden 1988). A greater amount of angular momentum acquired by low-density peaks (with respect to the high-density ones) implies that these peaks can more easily resist gravitational collapse and consequently it is more difficult for them to form structure, and in some conditions the structure formation by low mass peaks is even inhibited¹⁰.

The break of the self-similarity of the L-T relation may have also important consequences for determining the cluster masses from their luminosity. As shown by Shimizu et al. (2003), the predicted L-T relation is very sensitive to the assumed M-T relation, and then the non self-similarity of the L-T relation is strictly connected to that in the M-T relation. Also the M-T relation, as previously discussed, is non self-similar, and this behaviour has been interpreted in different ways (see introduction).

In Del Popolo 2002b, the bent in the M-T relation is entirely justified in terms of cluster tidal interaction with the neighbouring ones, or in other terms it is strictly connected to the asphericity of clusters (see Del Popolo & Gambera 1999 for a discussion on the relation between angular momentum acquisition, asphericity and structure formation). Non-sphericity introduces an asymmetric bent, dependent on mass, in the M-T relation that gives rise to a different slope at the low mass end ($T \sim 3\text{keV}$): the lower the mass the larger the bent.

The previous result is in agreement with AC result. In that paper, the authors used a nearly spherical collapsing region to obtain the M-T relation. According to their results, non-sphericity introduces an asymmetric, mass-dependent scatter (the lower the mass, the larger the scatter) for the M-T relation, thus altering the slope at the low masses end ($T \simeq 3\text{keV}$).

¹⁰One interesting point to mention, at this point, is that several different assumptions are able to reproduce the observed L-T. This could mean that L-T relation, is not a very sensitive test: since almost any change to the “pure” self-similar model, reproduces this relation.

As commented in the introduction, heating/cooling mechanisms are not necessary to explain the observational L-T correlation. Bryan & Norman (1998), carrying out large hydrodynamical simulations that followed the hierarchical evolution of clusters of galaxies, found that the observed M-T, L-T relations can be thoroughly reproduced if the number of particles and the spatial resolution are large enough. The importance of the numerical accuracy proves to be crucial to determining those relations, and so, for example, Mwanwong et al. (2001) using simulations with only 160^3 particles and a spatial resolution of $100h^{-1}$ Mpc, obtain that $L \propto T^2$ independent of mass, if radiative cooling is not implemented. In contrast, Bryan & Norman (1998), using simulations with 512^3 particles and a spatial resolution of $50h^{-1}$ Mpc, did reproduce the observational bend of the L-T relation at the low-mass region.

A priori, it is unclear why the L-T and M-T relations are that sensitive to resolution. One possible explanation goes in the direction of the results shown in this paper. Taking into account that proto-structures gain angular momentum owing to tidal interactions with other non-spherical structures, low resolution may hinder the gain of angular momentum by preventing an accurate determination of the proto-structure shape. To clarify this point, we shall use the simulations of Mwanwong et al. (2001) and Bryan & Norman (1998) as an example. The particle mass, m_p , of the first was $m_p = 2.1 \times 10^{10}h^{-1}M_\odot$, whereas the later used $m_p \simeq 6 \times 10^8h^{-1}M_\odot$ in their simulations. Since a common characteristic of hydro-dynamical calculations is that all particles have the same mass, clusters with $kT < 2$ keV (where the bend in the L-T relation starts to depart clearly from self-similarity) have masses of $M \sim 3 \times 10^{14}h^{-1}M_\odot$, i.e, they contain approximately $N < 1.4 \times 10^4$ and $N < 5 \times 10^5$ particles in Mwanwong et al. (2001) and Bryan & Norman (1998) simulations, respectively. As we go to lower masses, we reduce the number of particles enclosed in proto-structures. As a consequence, the shape and, therefore, the inertia axes, may fluctuate randomly, which would lead in average to a systematical decrease of angular momentum gained by low-mass proto-clusters.

Besides the poorly determined shape of low-mass structures, one must also take into account the possible effects of force resolution. In a typical N-Body evolution code, like for example the Treecode of L. Hernquist (1987), the force acting on a particle is given by the sum of two components: the force coming from the nearest neighbours and that coming from an expansion of the gravitational potential of the entire system up to quadrupole terms. As can be shown, the value of the average stochastic force in the simulation, F_{sim} , is an order of magnitude bigger than that obtained from the theory, F_{th} , of

stochastic forces. As a consequence only the higher force are taken into account, while the small fluctuations induced by the small scale substructure are not "seen". This is the case for CDM models in which the stochastic force generators are substructures at least three orders of magnitude smaller in size than the proto-structures in which they are embedded (e.g. clusters of galaxies).

Taking into account the large simulations required to obtain a good description of the L-T relation, it is not surprising that similar disagreements are reported in other cases too. For example, in the case of the M-T relation, it is noted that the results from different observational methods of mass measurements are not consistent with one another and with the simulation results (e.g., Horner, Mushotzky, & Scharf 1999, hereafter HMS; Neumann, & Arnaud 1999; Nevalainen, Markevitch, & Forman 2000, FRB). In general, X-ray mass estimates are about 80% lower than the predictions of hydro-simulations. On the other hand, X-ray mass estimates lead to normalisations about 50% higher than our result and simulations.

One possible source for difference between theoretical and observational normalisations is that the values for $\tilde{\beta}^{11}$ are different in the two cases due to systematic selection effects. Also, intriguingly, Bryan & Norman (1998) showed that there is a systematic increase in the obtained value of $\tilde{\beta}$ by increasing the resolution of the simulations.

We would like to stress that even **if** the effects of angular momentum are not taken into account, this last process gives rise to self-similar structures only in a first approximation. In fact: (a) the effective spectral index n_{eff} of CDM models depends, even if weakly, from the scale, going from values of $n_{\text{eff}} \simeq -1.2$ for clusters to $n_{\text{eff}} \simeq -2$ for galaxies; (b) we live in a universe with cosmological constant different from zero, which means that there is a typical redshift at which it became important for cosmic dynamics; (c) even dark matter profiles are not perfectly self-similar, since they depends on the concentration parameter, which in turn is inversely proportional with mass, this because smaller structures formed, on average, at earlier times, when cosmic density was larger.

As reported, Fig. 1 shows a slight difference between the SMMS prediction and that of PEM, being the slope predicted by SMSS, at low temperatures less steep than that of PEM, and MPEM. The difference is not so large, implying a difference in luminosity of 10% (larger for SMSS with respect to PEM). Also in Fig. 1, it is plotted the L-T relation predicted by MPEM. In this last case, the bending is produced by two effects: the threshold effect of the pre-heating temperature $kT_1 \simeq 0.5$ keV (as in CMT99) and to the effect of angular

¹¹ $\tilde{\beta} = \beta[1 + f(1/\beta - 1)\Omega_b/\Omega_m]$, where f is the fraction of the baryonic matter in the hot gas, and Ω_b is the density parameter of the baryonic matter.

momentum acquired by clusters. As a consequence, if we compare MPEM with PEM (or MSSM), the bending is larger (beside the threshold effect we have the acquisition of angular momentum).

Relative to this last item, looking at Fig. 1, one can see that the curve obtained from MSSM is very different to that corresponding to SSM, whereas the one from MPEM differs not much to that of PEM. The reason is the following: if we consider a cluster, without implementing pre-heating, the angular momentum acquisition is responsible for the slowing down and eventual stopping of the matter collapse towards the centre of the cluster, leading to the discussed consequences. Implementing pre-heating, this gives rise (by heating the uncondensed gas and therefore making it harder to compress in the core) to a region at higher temperature and pressure that acts like a boundary for the infalling gas which, therefore, reduces the effects induced by angular momentum acquisition.

In Fig. 2, we plot the results for the MPEM model: the average L-T correlation with the 2σ dispersion (dotted lines), for a tilted cosmogony. Group data from Ponman et al. (1996) are represented by solid squares while cluster data from Markevitch (1998) are represented by solid hexagons. The L-T correlation is given by the double convolution (Eq. (10)), while ΔL is obtained by Eq. (11). The normalisation has been fitted on the data (see CMT99).

The quantities and profiles of the PEM model are the same of CMT99, namely the reference cluster has a mass $m = M/M_0$, and a dark matter potential $\phi(r)$ as described in Appendix B. The density and temperature profiles are given by Eq. (30) and they should match the shock boundary conditions at the position $r_2 \simeq R_{\text{vir}}$. The average value and scatter of the parameter β , given by Eq. (31), calculated through the PEM and shown in Fig. 2 of CMT99, increases from $\beta = 0.5$ to $\beta \simeq 0.9$ while the baryonic fraction f_2 is the one in Fig. 3 of CMT99. The γ parameter is fixed as described in Appendix B. As the plot shows, in agreement with CMT99, the correlation is not a simple power law, but it starts as $L \propto T^2$ for very rich clusters, and after it bends down with decreasing T. As previously told, the bending is induced by two **mechanisms: the threshold imposed by the pre-heating temperature $kT_1 \simeq 0.5$ keV (as in CMT99) and the angular momentum acquired by clusters**. As a consequence, if we compare MSSM with PEM, the bending is larger (beside the threshold effect we have the acquisition of angular momentum).

We want to point a similitude between the role of pre-heating temperature, T , in the PEM and **that of the** angular momentum \mathcal{L} in our model. In the PEM, the thermal energy of infalling gas comes initially from stellar pre-heating (of nuclear origin); then it is increased to the virial value (of gravitational origin) when the accreted gas is bound to DM sub-clumps. So the pre-heating sets an effective threshold $kT_1 \sim 0.5$ keV to gas inclusion, which breaks the self-similar correlation $L \propto T^2$ not only in its vicinity but also up to a few keV. Increasing

the pre-heating temperature the bending in the L-T relation becomes more pronounced. A similar process occurs if the acquired angular momentum is larger.

A similar fitting formula to that of CMT98, for the predicted L-T correlation (for $T > T_1 \simeq 1$ keV), is given by:

$$\begin{aligned} L &= a_L T^{2+\alpha_L} (\rho/\rho_o)^{1/2} \\ a_L &\propto \Omega_0^{0.3} (1+z)^{0.22/\Omega_0} + (1-\Omega_0) e^{-0.7(1+z)} \\ \alpha_L &= a_1 (1+z)^{-0.2} e^{-a_2 (T-T_1)/\Omega_0^{0.1} (1+z)^{0.5}}, \end{aligned} \tag{12}$$

where the luminosity is expressed in units of 10^{44} erg/s and the temperature in keV, and with $a_1 = 1.2$ and $a_2 = 0.17$.

At temperatures larger than the threshold $kT_1 \simeq 0.5$ keV, the relative $\Delta L/L$ remains constant around 25%. A study of the dependence of $\langle L \rangle$ and ΔL on Ω_0 shows that both these quantities increase with increasing Ω_0 , similarly to what shown in CMT99¹²

Fig. 3, shows MSSM compared with observational data. Similarly to Fig. 2, we plot the average L-T correlation with the 2σ dispersion (dotted lines), for a tilted cosmogony. Group data from Ponman et al. (1996) are represented by solid squares while cluster data from Markevitch (1998) are represented by solid hexagons. The L-T correlation can be fitted in this case by a similar formula to that of Eq. (13), with $a_1 = 1.28$ and $a_2 = 0.19$. As reported, Fig. 1 shows a slight difference between the SMSS prediction and that of PEM, being the slope predicted by SMSS, at low temperatures less steep than that of PEM. The difference is not so large, implying a difference in luminosity of 10% (larger for SMSS). The fit to data of SMSS model, as Fig. 3 shows, is also very good.

To summarise, the key idea of the SMSS model and of other mechanisms proposed to reproduce the non-self-similarity of the L-T relation is in all cases fairly similar: If one wants to have clusters less luminous than SSM prediction, it is necessary to have a physical process that reduces the quantity of gas infalling towards the centre of the cluster which, therefore, reduces the core luminosity. **In the case of heating/cooling models, some energy input pre-heats the gas before it falls into new groups and clusters, hindering its flow into the latter. In the SMSS model, that role is played by the initial spin present in proto-clusters.**

¹²This is because the underlying strength of the current shocks grows on average as the merging rate (moderately) increases on approaching the critical cosmology, see Lacey & Cole (1993).

4. Conclusions

In this paper we showed that the presence of angular momentum during the collapse of a proto-structure leads to a non-self-similar L-T relation. The quoted effect leads, in X-rays, to a luminosity-temperature relation that scales as $L \propto T^5$, at scale of groups, flattening to $L \propto T^3$ for rich clusters and converging to $L \propto T^2$ at higher temperatures.

These results are in disagreement with the largely accepted assumption that heating/cooling processes and similar are fundamental in the originating the non-self similar behaviour (shaping) of the L-T relation. **As Bryan & Norman (1998) showed, it is not necessary to hypothesise pre-heating/cooling models in order to reproduce observations, on the contrary, it is possible to reproduce the observed L-T relation if the spatial and mass resolution are accurate enough. Poorly resolved clusters, with few particles enclosed, lead to self-similar L-T curves.**

We have shown that the large bend of the L-T relation is caused by the fact that the angular momentum acquired by a shell centred on a peak in the CDM density distribution is anti-correlated with density: high-density peaks acquire less angular momentum than low-density peaks. A greater amount of angular momentum acquired by low-density peaks (with respect to the high-density ones) implies that these peaks can more easily resist gravitational collapse and consequently it is more difficult for them to form structure. This results in a tendency for less dense regions to accrete less mass with respect to a classical spherical model. As a consequence, the X-ray luminosities of low-temperature clusters are small because their gas is less centrally concentrated than in hotter clusters.

REFERENCES

- Afshordi N., Cen R., 2001, astro-ph/0105020
- Allen S.W., Fabian A. 1998, MNRAS 297, L57
- Allen S.W., Schmidt R.W., Fabian A.C., 2001, MNRAS 328, 37
- Audit E., Teyssier R., Alimi J. M., 1997, A&A 325, 439
- Balogh M.L., Babul A., Patton D.R., MNRAS 307, 463
- Bardeen J.M., Bond J.R., Kaiser N., Szalay A.S., 1986, ApJ 304, 15
- Barnes J., Efstathiou G., 1987, ApJ, 319, 575

- Barrow J.D., Silk J., 1981, ApJ 250, 432
- Bialek J.J., Evrard A.E., Mohr J.J., 2001, ApJ 555, 597, (astro-ph/0010584)
- Bond J.R., Myers S.T., 1993a, preprint CITA/93/27
- Bond J.R., Myers S.T., 1993b preprint CITA/93/28
- Borgani et al. 2001, ApJ 559, L71
- Bower R.G., Castander F.J., Couch W., Ellis R.S., Böhringer H., 1997, MNRAS 291, 353
- Bryan G.L., Norman M.L., 1998, ApJ 495, 80, (astro-ph/9710107)
- Bryan G.L., ApJ 544, L1-L5
- Carlberg R.G., Yee H.K.C., Ellingson E., 1997, ApJ 478, 462
- Catelan P., Theuns T., 1996, MNRAS, 282, 436
- Cavaliere A., Menci N., Tozzi P., 1997, ApJ 484, 21
- Cavaliere A., Menci N., Tozzi P., 1998, ApJ 501, 493
- Cavaliere A., Menci N., Tozzi P., 1999, MNRAS 308, 599
- David L. P., Slyz A., Jones C., Forman W., Vrtilik S.D., 1993, ApJ, 412, 479
- David L.P., Jones C., Forman W., 1995, ApJ 445, 578
- Davis M., Peebles P.J.E., 1977, ApJS 34, 425
- Del Popolo A., Gambera M., 1998, A&A 337, 96
- Del Popolo A., Gambera M., 1999, A&A 344, 17
- Del Popolo, A., E. N. Ercan, Z. Q. Xia, 2001, AJ 122, 487
- Del Popolo A., 2002a A&A 387, 759
- Del Popolo, A., 2002b, MNRAS 336, 81
- Edge A.C., Stuart G.C., 1991, MNRAS 252, 414
- Efstathiou G., Jones B.J.T., 1979, MNRAS, 186, 133
- Eisenstein D.J., Loeb A., 1995, ApJ, 439, 520

- Eke V.R., Cole S., Frenk C.S., 1996, MNRAS 282, 263
- Evrard A.E., Henry J.P., 1991, ApJ 383, 95
- Evrard A.E., Metzler C.A., Navarro J.F., 1996, ApJ 469, 494
- Finoguenov A., Reiprich T.H., Böeringer H., 2001, A&A 368, 749
- Gioia I., Henry J.P., Maccacaro T., Morris S.L., Stocke J.T., Wolter A., 1990, ApJ 356, 35
- Henry J.P., Gioia I., Maccacaro T., Morris S.L., Stocke J.T., Wolter A., 1992, ApJ 386, 408
- Hernquist L., 1987
- Hjorth J., Oukbir J., van Kampen e., 1998, MNRAS 298, L1
- Hiotelis N., 2002, A& A, 382,84
- Hoffman Y., 1986, ApJ 301, 65
- Horner D.J., Mushotzky R.F., Scharf C.A., 1999, Apj 520, 78
- Kaiser N., 1986, MNRAS 222, 323
- Kaiser N., 1991, ApJ 383, 104
- Kitayama T., Suto Y., 1996, ApJ 469,480
- Kratsov A.V., Klypin A.A., Bullock J.S., Primack J.R., 1998, ApJ, 502,48
- Lacey C., Cole S., 1993, MNRAS 262, 627
- Lokas E.L., Juskiewicz R., Bouchet F.R., Hivon E., 1996, ApJ 467, 1
- Markevitch M., 1998, Apj 503, 77
- Mathiesen B.F., Evrard A.E., 2001, astro-ph/0004309 (ApJ, in press)
- Mathiesen B.F., 2001, MNRAS 326, 1, (astro-ph/0012117)
- Muanwong O., Thomas P. A., Kay S. T., Pearce F. R., Couchman H. M. P., 2001, ApJ 552, 27, (astro-ph/0102048)
- Navarro J.F., Frenk C.S., White S.D.M., 1995, MNRAS 275, 720
- Navarro J.F., Frenk C.S., White S.D.M., 1997, ApJ 490, 493

- Neumann D.M., Arnaud M., 1999, A&A 348, 711
- Nevalainen J., Markevitch M., Forman W., 2000, ApJ 532, 694
- Pearce F.R., Thomas P.A., Kay S.T., Pearce F.R., Couchman H.P.M., ApJ 552, L27-L30
- Peebles, P.J.E., 1971, A&A, 11, 377
- Peebles P.J.E., Groth E.J., 1976, A&A 53, 131
- Peebles P.J.E., 1990, ApJ 365, 27
- Peebles, P.J.E., 1993, Principles of Physical Cosmology, Princeton University Press
- Perrenod S.C. 1980, ApJ 236, 373
- Ponman T.J., Cannon D.B., Navarro J.F., 1999, Nature 397, 135
- Renzini A., 1997, ApJ 488, 35
- Ryden B.S., 1988, ApJ 329, 589
- Sarazin C.L., 1988, X-ray emission from Clusters of Galaxies (Cambridge: Cambridge University Press)
- Shimizu M., Kitayama T., Sasaki S., Suto Y., 2003, ApJ 590, 197
- Steinmetz M., Bartelmann M., 1995, MNRAS, 272, 570
- Szalay A.S., Silk J., 1983, ApJ 264, L31
- Takizawa M., Mineshige S., 1998, ApJ 499, 82
- Thomas P.A., 1998
- Thomas P.A., Muanwong O., Kay S.T., Liddle A.R., 2001, astro-ph/0112449
- Tozzi P., Norman C. 2001, ApJ 546, 63
- Viana P.T.P., Liddle A.R., 1996, MNRAS 281, 323
- Villumsen J.V., Davis M., 1986, ApJ 308, 499
- Voglis N., Hiotelis N., 1989, A&A, 218, 1
- Voit C. M., Donahue M., 1998, ApJ 500, 111 (astro-ph/9804306)

Voit C. M., 2000, ApJ 543, 113 (astro-ph/0006366)

Voit M., Bryan G. 2001, Nature 414, 425

Warren M.S., Quinn P.J., Salmon J.K., Zurek W.H., 1992, ApJ,399,405

White R.E., 1991, ApJ 367, 69

Wu K.K.S., Fabian A.C., Nulsen P.E.J, 2000, MNRAS 308, 599

Xu H., Jing G., Wu X., 2001, ApJ 553, 78, (astro-ph/0101564)

5. Appendix A: M-T relation

As previously quoted, numerical methods and simple scaling arguments suggest that the X-ray temperature of clusters, T_X , can be directly related to their masses as $M_{\text{vir}} \propto T_X^{3/2} \rho_b^{-1/2} \Delta_{\text{vir}}^{-1/2}$, where ρ_b is the critical density, Δ_{vir} the mean density within the virial radius R_{vir} .

In Del Popolo & Gambera (1999) and Del Popolo (2002), we got the M-T relation in two different ways: (1) modifying the top-hat model; (2) modifying Voit & Donahue (1998) (hereafter V98) model.

In the first, we modified the top-hat model in order to take account of angular momentum acquisition by protostructures and used a modified version of the virial theorem in order to include a surface pressure term (V2000, AC). This correction is due to the fact that at the virial radius R_{vir} the density is non-zero and this requires a surface pressure term to be included in the virial theorem (Carlberg, Yee & Ellingson 1997) (the existence of this confining pressure is usually not accounted for in the top-hat collapse model). The derivation of the previous relation is fundamentally based on the approximation of cluster formation with the evolution of a spherical top-hat density perturbation (Peebles 1993) and on the additional assumption that each cluster observed at a redshift z has just reached the moment of virialization. This last assumption is currently known as the late-formation approximation, which is a good one in a critical $\Omega_0 = 1$, because for this value of Ω massive clusters develop rapidly at all redshifts and the moment of virialization is always close to that of observation. In other terms for $\Omega_0 = 1$, the accretion rate remains sufficiently high, and this implies that the clusters we actually observe attained their observed masses recently. In the $\Omega_0 < 1$ case cluster formation is “shutting down” and it is necessary to take account of the differences between the moment of virialization and that of observation. The problem becomes worse going through $\Omega_0 \ll 1$: in fact in the late-formation approximation M_{vir} rises steadily since $\rho_b \Delta_{\text{vir}}$ declines indefinitely, while we expect that the cluster formation is going to stop ¹³.

The late-formation approximation is a good one for many purposes, but a better one can be obtained in the low- Ω limit. As can be found in the literature, there are two ways of improving the quoted model. One is to define a formation redshift z_f at which a cluster virializes and after the properties of observed clusters at z are obtained by integrating over the appropriate distribution of formation redshifts (Kitayama & Suto 1996; Viana & Liddle 1996). The second possibility is the one described by V98, V2000. In this approach, the top-hat cluster formation model is substituted by a model of cluster formation from spherically

¹³The result of the late-formation approximation is displayed in Eqs. 18-19 of Del Popolo (2002)

symmetric perturbations with negative radial density gradients. The fact that clusters form gradually, and not instantaneously, is taken into account in the merging-halo formalism of Lacey & Cole (1993). In hierarchical models for structure formation, the growth of the largest clusters is quasi-continuous since these large objects are so rare that they almost never merge with another cluster of similar size (Lacey & Cole 1993). So, Lacey & Cole (1993) approach extends the Press-Schechter formalism by considering how clusters grow via accretion of smaller virialized objects. Summarising, in order to obtain the proper normalisation and time evolution of the M-T relation, one has to account:

- a) for the continuous accretion of mass of clusters;
- b) for the non-zero density at R_{vir} , requiring a change in the virial theorem by including a surface pressure term.

The M-T relation derived by means of a model of continuous accretion, differs from the late-formation model in both normalisation and time-dependent behaviour.¹⁴

In order to obtain the M-T relation in this second approach, we assume, as shown by V2000, the mass grows like $M \propto \omega^{-3/(n+3)}$ (Lacey & Cole 1993; V98; V2000). The virial energy of the cluster, $-E$, can be calculated by integrating the

In order to obtain an expression for the kinetic energy, we firstly calculated E/M :

$$\frac{E}{M} = -\frac{\int \epsilon dM}{M} = \frac{3m_1}{10(m_1 - 1)} \left(\frac{2\pi G}{t_\Omega} \right)^{\frac{2}{3}} M^{\frac{2}{3}} \left[\frac{1}{m_1} + \left(\frac{t_\Omega}{t} \right)^{\frac{2}{3}} + \frac{K_1(m_1, x)}{M^{8/3}} \right] \quad (13)$$

$$K_1(m_1, x) = (m_1 - 1) FxLerchPhi(x, 1, 3m_1/5 + 1) - (m_1 - 1) FLerchPhi(x, 1, 3m_1/5) \quad (14)$$

¹⁴A comparison of the normalisation predicted by the late-formation model with that predicted by simulations of Evrard, Metzler & Navarro (1996) shows that when $\Omega_0 = 1$ this normalisation is only 4% below the empirical value, but it lies 20% below it for $\Omega_0 = 0.2$. In the case of V2000 model and for a power-law spectrum, a comparison with the same simulations show that the temperature normalisation of the $n = -2$ case deviates by less than 10% over the range $0.2 < \Omega_0 < 1$ and by $\simeq 18\%$ in the case $n = -1$ (V2000). The normalisation obtained by the V2000 model, even if it is more accurate than that given by the late formation, or that by AC which is in agreement with hydro-simulations, show a noteworthy discrepancy when compared with X-ray mass estimates (about 50% for the AC model; see also V2000). One possible source for differences in theoretical and observational normalisations may be due to the fact that β is different in the two cases because of systematic selection effects. For example, as shown by Bryan & Norman (1998), increasing the resolution of simulations there is an increase in the value of β . So summarising, for what concerns normalisation, the continuous formation model gives more precise results than the late formation one, but in any case if we want to fit observations we need to shift the normalisation (see AC).

where,

$$F = \frac{2^{7/3} \pi^{2/3} \xi \rho_b^{2/3}}{3^{2/3} H^2 \Omega} \int_0^r \frac{\mathcal{L}^2 dr}{r^3} \quad (15)$$

$m_1 = 5/(n+3)$, $t_\Omega = \frac{\pi \Omega_0}{H_0(1-\Omega_0-\Omega_\Lambda)^{3/2}}$, $x = 1 + (\frac{t_\Omega}{t})^{2/3}$ which is connected to mass by $M = M_0 x^{-3m_1/5}$ (V2000) and $\xi = \frac{r_{ta}}{x_1}$, where r_{ta} is the turn-around radius and x_1 is defined by the relation $M = \frac{4\pi \rho_b x_1^3}{3}$ with ρ_b is the background density. The *LerchPhi* function is defined as follows:

$$LerchPhi(z, a, v) = \sum_{n=0}^{\infty} \frac{z^n}{(v+n)^a} \quad (16)$$

The angular momentum, \mathcal{L} , acquired by the protostructure, is calculated using the same model (and same spectrum) as described in Del Popolo & Gambera (1998, 1999). More hints on the model and some of the model limits can be found in Del Popolo, Ercan & Gambera (2001)). Then, the virial theorem with the surface pressure term correction, as in V2000, is used in order to get a connection between the kinetic energy and temperature. We utilise the usual relation:

$$\langle K \rangle = \frac{3\tilde{\beta} M k T}{2\mu m_p} \quad (17)$$

(AC), where k is the Boltzmann constant, $\mu = 0.59$ is the mean molecular weight, m_p the proton mass and $\tilde{\beta} = \frac{\sigma_v^2}{kT/\mu m_p}$, being σ_v the mass-weighted mean velocity dispersion of dark matter particles, and $\tilde{\beta} = \beta[1 + f(1/\beta - 1)\Omega_b/\Omega_m]$, where f is the fraction of the baryonic matter in the hot gas, and Ω_b is the density parameter of the baryonic matter. In this way, we finally get:

$$kT = \frac{2}{5} a \frac{\mu m_p}{2\beta} \frac{m_1}{m_1 - 1} \left(\frac{2\pi G}{t_\Omega} \right)^{\frac{2}{3}} M^{\frac{2}{3}} \left[\frac{1}{m_1} + \left(\frac{t_\Omega}{t} \right)^{\frac{2}{3}} + \frac{K_1(m_1, x)}{M_0^{8/3}} \right] \quad (18)$$

where $a = \frac{\bar{\rho}}{2\rho(R_{vir})-\bar{\rho}}$ is the ratio between kinetic and total energy (V2000). If $K_1 = 0$, Eq. (13) reduces to Eq. (10) of V2000. As stressed by V2000, some factors give rise to an higher value of E/M with respect the case of the late-formation value. The $m_1/(m_1 - 1)$ value which accounts for the effect of early infall. The $1/m_1$ value in the square bracket of Eq. (13) which accounts for the cessation of cluster formation when $t \gg t_\Omega$. Finally in Eq. (13) a new term is present, which comes from the tidal interaction.

Using the relation $\Delta_{vir} = \frac{8\pi^2}{H^2 t^2}$ (see V2000), and in the early-time limit: ($t \ll t_\Omega$), Eq. (18), reduces to:

$$kT = \frac{2}{5} \frac{m_1}{m_1 - 1} a \frac{\mu m_p}{2\beta} G M^{\frac{2}{3}} \left(\frac{4\pi}{3} \rho_b \Delta_{vir} \right)^{1/3} \quad (19)$$

which, in the case $n \sim -2$, $a \sim 2$ is identical to the late-formation formula, described in V2000 (see their Eq. (8)). Normalising Eq. (18) similarly to V2000, we get:

$$kT \simeq 8keV \left(\frac{M^{\frac{2}{3}}}{10^{15} h^{-1} M_{\odot}} \right) \frac{\left[\frac{1}{m_1} + \left(\frac{t_{\Omega}}{t} \right)^{\frac{2}{3}} + \frac{K_1(m_1, x)}{M^{8/3}} \right]}{\left[\frac{1}{m_1} + \left(\frac{t_{\Omega}}{t_0} \right)^{\frac{2}{3}} + \frac{K_0(m_1, x)}{M_0^{8/3}} \right]} \quad (20)$$

where $K_0(m_1, x)$ indicates that $K_1(m_1, x)$ must be calculated assuming $t = t_0$

Eq. (20) when compared to the result of V2000 (Eq. 17) shows an additional term, mass dependent. This means that, as in the case of the top-hat model, the M-T relation is no longer self-similar showing a break at the low mass end (see next section).

6. Appendix B: L-T relation in the MPEM

The X-ray bolometric luminosity of a cluster is given by Eq. (1), which in CMT98 notation is:

$$L \propto \int_0^{r_2} n^2(r) T^{1/2}(r) d^3r . \quad (21)$$

Here $T(r)$ is temperature in the plasma and r_2 is the cluster boundary, that we take to be close to the virial radius $R_{\text{vir}} \propto M^{1/3} \rho^{-1/3}$, where $\rho(z) \propto (1+z)^3$ is the DM density in the cluster, proportional to the average cosmic DM density $\rho_u(z)$ at formation. The infalling gas is expected to become supersonic near r_2 (see, e.g., Perrenod 1980; Takizawa & Mineshige 1998) so that a shock front will form there. The conservations across the shock of mass, energy and stresses yield the Rankine-Hugoniot conditions, i.e., the temperature and density jumps from the outer values T_1 and n_1 to T_2 and n_2 just interior to r_2 . Then the luminosity may be rewritten in the form

$$L \propto r_2^3 n_2^2 T_2^{1/2} \int_0^1 d^3x \left[\frac{n(x)}{n_2} \right]^2 \left[\frac{T(x)}{T_2} \right]^{1/2} , \quad (22)$$

where $x \equiv r/r_2$. n_1 is fixed by $n_1 \propto f_u \rho_u / m_p$, in terms of the universal baryonic fraction f_u ; whereas T_1 is determined only statistically, through the diverse merging histories ending up in the mass M . In sum, a given dark mass M admits a set of ICP equilibrium states characterized by different boundary conditions, each corresponding to a different realization of the dynamical merging history. It is the convolution over such set which provides the average values of L and R_X , and their scatter. Following CMT98, the pre-shock temperature in a merging event is that of the infalling gas, and if the latter is contained in a sufficient deep potential well, T_1 is the virial temperature $T_{1v} \propto \Delta m / r$ of the secondary merging partner;

on using $r \propto (\Delta m/\rho)^{1/3}$ this writes

$$k T_{1v} = 4.5 (\Delta m)^{2/3} (\rho/\rho_o)^{1/3} \text{ keV}, \quad (23)$$

where the numerical coefficient is taken from Hjorth, Oukbir & van Kampen (1998), and the masses $m = M/M_0$ are normalised to the current value $M_0 = 0.6 \times 10^{15} \Omega_0 h^{-1} M_\odot$ (i.e., the mass enclosed within a sphere of $8h^{-1}$ Mpc), so in the following the actual value of T_1 will be

$$T_1 = \max [T_{1v}, T_{1*}]^{15} \quad (24)$$

Given T_1 , the boundary conditions for the ICP in the cluster is set by the strength of the shocks separating the inner from the infalling gas. In the case of three degrees of freedom and for a nearly hydrostatic post-shock condition with $v_2 \ll v_1$, assuming the shock velocity to match the growth rate of the virial radius $R_{\text{vir}}(t)$:

$$kT_2 = \frac{\mu m_p v_1^2}{3} \left[\frac{(1 + \sqrt{1 + \epsilon})^2}{4} + \frac{7}{10} \epsilon - \frac{3}{20} \frac{\epsilon^2}{(1 + \sqrt{1 + \epsilon})^2} \right]. \quad (25)$$

Cavaliere, Menci e Tozzi (1997) (CMT97).

Here $\epsilon \equiv 15kT_1/4\mu m_p v_1^2$ and μ is the average molecular weight; the inflow velocity v_1 is set by the potential drop across the region of nearly free fall, to read $v_1 \simeq \sqrt{-\phi_2/m_p}$ in terms of the potential ϕ_2 at r_2 . In the case of strong shocks, appropriate to “cold inflow”, $\epsilon \ll 1$, as in rich clusters accreting small clumps and diffuse gas, the approximation

$$kT_2 \simeq -\phi_2/3 + 3kT_1/2 \quad (26)$$

holds, where ϕ_2 is the gravitational potential energy at $r_2 \simeq R_{\text{vir}}$. For $\epsilon \geq 1$ the shock is weak, and $T_2 \simeq T_1$. From T_2 and T_1 , the density jump at the boundary n_2/n_1 is found to read (see CMT97)

$$\frac{n_2}{n_1} = 2 \left(1 - \frac{T_1}{T_2} \right) + \left[4 \left(1 - \frac{T_1}{T_2} \right)^2 + \frac{T_1}{T_2} \right]^{1/2}. \quad (27)$$

Adopting the polytropic temperature description $T(x)/T_2 = [n(x)/n_2]^{\gamma-1}$, with the index γ in the range $1 \leq \gamma \leq 5/3$, and that the radius r_2 may be written in terms of temperature $T_v \propto m/r_2$ and that $m \propto \rho r_2^3$, leading to $r_2 \propto (t/\rho)^{1/2}$, the luminosity can be written in the form:

¹⁵An independent lower bound $kT_{1*} \approx 0.5$ keV is provided by preheating of diffuse external gas, due to feedback energy inputs following star formation and evolution all the way to supernovae (David et al. 1995; Renzini 1997).

$$L \propto \left(\frac{n_2}{n_1}\right)^2 m T_v^{1/2} \rho \left[\frac{T_2}{T_v}\right]^{1/2} \frac{1}{[n(r)/n_2]^{2+(\gamma-1)/2}}, \quad (28)$$

where the bar denotes the integration over the emitting volume $r^3 \leq r_2^3$, and ρ is the average DM density in the cluster, proportional to ρ_u and so to n_1 .

Eq. (28) can be also cast in the form:

$$L \propto \left(\frac{n_2}{n_1}\right)^2 \rho \left[\frac{T_2}{T_v}\right]^{1/2} \frac{1}{[n(r)/n_2]^{2+(\gamma-1)/2}} m^{4/3} \sqrt{\frac{\frac{1}{m_1} + \left(\frac{t_\Omega}{t}\right)^{2/3} + \frac{K}{\left(\frac{m}{m_o}\right)^{8/3}}}{\frac{1}{m_1} + \left(\frac{t_\Omega}{t}\right)^{2/3} + \frac{K_0}{m_o^{8/3}}}} \quad (29)$$

The ratio $n(x)/n_2$ is obtained from the hydrostatic equilibrium $dP/m_p n dr = -G M(< r)/r^2 = -d\phi/dr$ with the polytropic pressure $P(r) = kT_2 n_2 [n(r)/n_2]^\gamma$. This yields (see Cavaliere & Fusco Femiano 1978; Sarazin 1988, and bibliography therein) the profiles

$$\frac{n(r)}{n_2} = \left[\frac{T(r)}{T_2}\right]^{1/(\gamma-1)} = \left\{1 + \frac{\gamma-1}{\gamma} \beta [\tilde{\phi}_2 - \tilde{\phi}(r)]\right\}^{1/(\gamma-1)}, \quad (30)$$

where $\tilde{\phi} \equiv \phi/\mu m_p \sigma_2^2$ is the potential normalised to the associated one-dimensional DM velocity dispersion at r_2 . The ICP disposition in eq. (11) relative to the DM depends on the parameter, already met previously:

$$\beta = \mu m_p \sigma_2^2 / k T_2, \quad (31)$$

and is further modulated by the second parameter γ , to yield as the latter increases flatter profiles $n(r)$ and steeper $T(r)$.¹⁶

The function $\beta(T)$ can be easily computed from Eq. (26) for a given dark matter potential ϕ_2 corresponding to $\rho(r)$. $\phi(r)$ and $\sigma(r)$ are obtained in agreement with Navarro, Frenk & White (1997).

¹⁶For the King potential (see Sarazin 1988) and CMT97, with core radius $r_c = R_v/12$, $\beta(T)$ increases from $\beta \simeq 0.5$, for $T \simeq T_1$ to $\beta \simeq 0.9$ for $T \gg T_1$. A similar result is obtained for a Navarro et al (1996) potential. The other parameter γ will be bounded according to CMT99, The polytropic index $\gamma \geq 1$ describes the equation of state for the ICP. An upper bound to it arises if the overall thermal energy of the ICP is not to exceed its gravitational energy. The thermal and the gravitational energy are computed using the profiles in Eq. (30), and their ratio is given in Fig. 4 of CMT99, to show that the *upper* bound $\gamma \leq 1.3$ holds. It turns out that observations by Markevitch et al. (1997) are consistent with the $T(r)$ predicted when $\gamma = 1.2 \pm 0.1$, in our allowed range. Hereafter we shall focus on $\gamma = 1.2$.

7. Appendix C: Calculation of the angular momentum

The effect of tidal torques on structures evolution has been studied in several papers especially in connection with the origin of galaxies rotation (Hoyle 1949; Peebles 1969; White 1984; Ryden 1988 (hereafter R88); Eisenstein & Loeb 1995).

Following Eisenstein & Loeb (1995), we separate the universe into two disjoint parts: the collapsing region, characterised by having high density, and the rest of the universe. The boundary between these two regions is taken to be a sphere centred on the origin. As usual, in the following, we denote with $\rho(\mathbf{x})$, being \mathbf{x} the position vector, the density as function of space and $\delta(\mathbf{x}) = \frac{\rho(\mathbf{x}) - \rho_b}{\rho_b}$. The gravitational force exerted on the spherical central region by the external universe can be calculated by expanding the potential, $\Phi(\mathbf{x})$, in spherical harmonics. Assuming that the sphere has radius R , we have:

$$\Phi(\mathbf{x}) = \sum_{l=0}^{\infty} \frac{4\pi}{2l+1} \sum_{m=-l}^l a_{lm}(x) Y_{lm}(\theta, \phi) x^l \quad (32)$$

where Y_{lm} are spherical harmonics and the tidal moments, a_{lm} , are given by:

$$a_{lm}(x) = \rho_b \int_R^{\infty} Y_{lm}(\theta, \phi) \rho(\mathbf{s}) s^{-l-1} d^3s \quad (33)$$

In this approach the proto-structure is divided into a series of mass shells and the torque on each mass shell is computed separately. The density profile of each proto-structure is approximated by the superposition of a spherical profile, $\delta(r)$, and a random CDM distribution, $\varepsilon(\mathbf{r})$, which provides the quadrupole moment of the proto-structure. To the first order, the initial density can be represented by:

$$\rho(\mathbf{r}) = \rho_b [1 + \delta(r)] [1 + \varepsilon(\mathbf{r})] \quad (34)$$

where $\varepsilon(\mathbf{r})$ is given by:

$$\langle |\varepsilon_k|^2 \rangle = P(k) \quad (35)$$

being $P(k)$ the power spectrum. The torque on a thin spherical shell of internal radius x is given by:

$$\tau(x) = -\frac{GM_{sh}}{4\pi} \int \varepsilon(\mathbf{x}) \mathbf{x} \times \nabla \Phi(\mathbf{x}) d\Omega \quad (36)$$

where $M_{sh} = 4\pi\rho_b [1 + \delta(x)] x^2 \delta x$. Before going on, I want to recall that we are interested in the acquisition of angular momentum from the inner region, and for this purpose we take account only of the $l = 2$ (quadrupole) term. In fact, the $l = 0$ term produces no force, while the dipole ($l = 1$) cannot change the shape or induce any rotation of the inner region. As

shown by Eisenstein & Loeb (1995), in the standard CDM scenario the dipole is generated at large scales, so the object we are studying and its neighbourhood move as bulk flow with the consequence that the angular distribution of matter will be very small, then the dipole terms can be ignored. Because of the isotropy of the random field, $\varepsilon(\mathbf{x})$, Equation (36) can be written as:

$$\langle |\tau|^2 \rangle = \sqrt{(30) \frac{4\pi G}{5}} \left[\langle a_{2m}(x)^2 \rangle \langle q_{2m}(x)^2 \rangle - \langle a_{2m}(x) q_{2m}^*(x) \rangle^2 \right]^{1/2} \quad (37)$$

where $\langle \rangle$ indicates a mean value of the physical quantity considered. As stressed in the next section, following Eisenstein & Loeb (1995), the integration of the equations of motion shall be ended at some time before the inner external tidal shell (i.e., the innermost shell of the part of the universe outside the sphere containing the ellipsoid) collapses. Then the inner region behaves as a density peak. This last point is an important one in the development of the present paper.

An important question to ask, before going on, regards the role of triaxiality of the ellipsoid (density peak) in generating a quadrupole moment. Equation (37) takes into account the quadrupole moment coming from the secondary perturbation near the peak. The density distribution around the inner region is characterised by a mean spherical distribution, δ , and a random isotropic field. In reality the central region is a triaxial ellipsoid. It is then important to evaluate the contribution to the quadrupole moment due to the triaxiality. Remembering that the quadrupole moments are given by:

$$q_{2m} = \int_{|\mathbf{r}| < R} Y_{2m}^*(\theta, \phi) s^2 \rho(\mathbf{s}) d^3 s = \frac{x^2 M_{\text{sh}}}{4\pi} \int Y_{2m}^*(\theta, \phi) \varepsilon(\mathbf{x}) d\Omega \quad (38)$$

and approximating the density profile as:

$$\delta(\mathbf{x}) = \langle \delta(x) \rangle_{\text{spherical}} + \nu f(x) A(e, p) \quad (39)$$

being $\langle \delta(x) \rangle_{\text{spherical}}$ the mean spherical profile, $\nu = \frac{\delta}{\sigma}$ the peak height and σ the r.m.s. value of δ . The function $A(e, p)$ of the triaxiality parameters, e and p , is given by:

$$A(e, p) = 3e(1 - \sin^2 \theta - \sin^2 \theta \sin^2 \phi) + p(1 - 3 \sin^2 \theta \cos^2 \phi) \quad (40)$$

while the function $f(x)$ is given (R88) by:

$$f(x) = \frac{5}{2\sigma} R_*^2 \left(\frac{1}{x} \frac{d\xi}{dx} - \frac{1}{3} \nabla^2 \xi \right) \quad (41)$$

where ξ , σ and R_* are respectively the two-point correlation function, the mass variance and a parameter connected to the spectral moments (see Bardeen et al. 1986, equation (4.6d),

hereafter BBKS). Substituting equation (39) and equation (40) in equation (38) it is easy to show that the sum of the mean quadrupole moments due to triaxiality is:

$$\frac{1}{M_{\text{sh}}} \sum_{m=-2}^2 \langle q_{2m}(x) \rangle = \nu x^2 f(x) \left(\frac{1}{2\pi} \sqrt{6\pi/5} (e - p) + \frac{1}{4\pi} \sqrt{4\pi/5} (3e + p) \right) \quad (42)$$

which must be compared with that produced by the secondary perturbations, ε :

$$\langle q_{2m}(x)^2 \rangle = \frac{x^4}{(2\pi)^3} M_{\text{sh}}^2 \int k^2 P(k) j_2(kx)^2 dk \quad (43)$$

where j_2 is the Bessel function of order 2. The values of e and p can be obtained from the distribution of ellipticity and prolateness (BBKS, equation (7.6) and figure 7) or for $\nu > 2$ by:

$$e = \frac{1}{\sqrt{5}x [1 + 6/(5x^2)]^{1/2}} \quad (44)$$

and

$$p = \frac{6}{5x^4 [1 + 6/(5x^2)]^2} \quad (45)$$

(BBKS equation (7.7)). where x is given in BBKS (equation (6.13)). In the case of a peak with $\nu = 3$, we have $e \simeq 0.15$, $p \simeq 0.014$ while for peaks having $\nu = 2$ and $\nu = 1$ they are respectively given by $e \simeq 0.2$, $p \simeq 0.03$ and $e \simeq 0.25$ $p \simeq 0.04$.

As shown in figure 1 of Del Popolo et al. (2001), for a 3σ profile, the source of quadrupole moment due to triaxiality is less important than that produced by the random perturbations ε in all the proto-structure, except in the central regions where the quadrupole moment due to triaxiality is comparable in magnitude to that due to secondary perturbations. In other words, the triaxiality has a significant effect only in the very central regions, which contains no more than a few percent of the total mass and where the acquisition of angular momentum is negligible. It follows that the triaxiality can be ignored while computing both expansion and spin growth (R88). Moreover, as observed by Eisenstein & Loeb (1995), the ellipsoid model does better in describing low shear regions (having higher values of ν), whose collapse is more spherical and then the effects of triaxiality are less evident. Just this peaks, having at least $\nu > 2$, shall be studied in this paper. In any case, even if the triaxiality was not negligible it should contribute to increment the acquisition of angular momentum (Eisenstein & Loeb 1995), and finally to a larger effect on the density evolution, (i.e., a larger reduction of the growing rate of the density).

In order to find the total angular momentum imparted to a mass shell by tidal torques, it is necessary to know the time dependence of the torque. This can be done connecting q_{2m} and

a_{2m} to parameters of the spherical collapse model (Eisenstein & Loeb 1995 (equation (32), R88 (equation (32) and (34)). Following R88 we have:

$$q_{2m}(\theta) = \frac{1}{4} q_{2m,0} \bar{\delta}_0^{-3} \frac{(1 - \cos \theta)^2 f_2(\theta)}{f_1(\theta) - \left(\frac{\delta_0}{\bar{\delta}_0}\right) f_2(\theta)} \quad (46)$$

and

$$a_{2m}(\theta) = a_{2m,0} \left(\frac{4}{3}\right)^{4/3} \bar{\delta}_0 (\theta - \sin \theta)^{-4/3} \quad (47)$$

The collapse parameter θ is given by:

$$t(\theta) = \frac{3}{4} t_0 \bar{\delta}_0^{-3/2} (\theta - \sin \theta) \quad (48)$$

Equation (46) and (47), by means of equation (37), give to us the tidal torque:

$$\tau(\theta) = \tau_0 \left(\frac{4}{3}\right)^{(1/3)} \bar{\delta}_0^{-1} \frac{(1 - \cos \theta)^2}{(\theta - \sin \theta)^{(4/3)}} \frac{f_2(\theta)}{f_1(\theta) - \left(\frac{\delta_0}{\bar{\delta}_0}\right) f_2(\theta)} \quad (49)$$

where $f_1(\theta)$ and $f_2(\theta)$ are given in R88 (Eq. 31), τ_0 and $\delta_0 = \frac{\rho - \rho_b}{\rho_b}$ are respectively the torque and the mean fractional density excess inside the shell, as measured at current epoch t_0 . The angular momentum acquired during expansion can then be obtained integrating the torque over time:

$$L = \int \tau(\theta) \frac{dt}{d\theta} d\theta \quad (50)$$

As remarked in the Del Popolo et al. (2001) the angular momentum obtained from equation(50) is evaluated at the time of maximum expansion t_M . Then the calculation of the angular momentum can be solved by means of equation (50), once we have made a choose for the power spectrum. With the power spectrum and the parameters given in the next section and for a $\nu = 2$ peak, the model gives a value of $2.5 \times 10^{74} \text{gcm}^2/\text{s}$. As previously quoted, we assume that from t_M on, the ellipsoid has this constant angular momentum. Following the procedures 1) and/or 2), we shall be able to get the time evolution of the density.
